Dislocation Kink Motion in Silicon

Y. M. Huang, J. C. H. Spence, and O. F. Sankey
Department of Physics, Arizona State University, Tempe, Arizona 85287
(Received 24 October 1994)

Ductility is controlled at the atomic level by dislocation kink motion. The migration energy for kinks on the 30° partial dislocation in silicon has been computed *ab initio* in agreement with experiment. The electronic structure changes from semiconducting to metallic at the saddle-point configuration. Band structure energy controls kink motion, so valence electrons control shearing motions involved with ductility, whereas tensile forces involved in fracture depend on both ion-ion and valence forces. Doping effects on dislocation mobility are explained.

PACS numbers: 61.72.Lk, 31.15.Ct, 34.20.Cf, 71.45.Nt

For millennia, man's ability to fashion useful objects has depended on the phenomenon of ductility. The fundamental atomic mechanisms which control ductility are based in turn on the dislocation and its kinks, those sites within a crystal where plastic deformation is identified with the motion of a single atom, according to accepted theory (Hirth and Lothe [1]). We report here the results of the first *ab initio* computation of the energetics of kink motion. The problem is akin to stress-induced diffusion without mass transport. The energy barriers to kink motion control the strength of the ductile materials, the temperature and orientation dependence of the critical resolved shear stress (failure of Schmid's law) and the phenomenon of lattice friction (which establishes a terminal velocity for dislocations) can only be explained in terms of the atomic structure of kinks. In metals, double kink nucleation energies exert a controlling influence, the energy barrier to kink migration is small, and studies based on atomic potentials have given a good understanding of general trends. For semiconductors, new effects such a photoplasticity and a dependence of dislocation mobility on doping appear [2]. Experiments suggest that kinks provide one of the electrically active sites on dislocations [3]. An understanding of all these issues depends crucially on the atomic and electronic structure associated with kink motion. Excellent reviews exist [4–6]. Current issues include charged kinks and antiphase defects (APD) [7,8], the shuffle-glide question [9], correlated kink motion [10], and the nature of impurity pinning centers [11]. For silicon at low temperatures the Peierls potential is rate controlling, and a consensus has emerged that the band gap is cleared of deep states by a Peierls-type reconstruction of both the common 30° and 90° partial dislocation cores [12,13]. We study here reconstructed kinks on the 30° Shockley partial dislocation on the (111) slip plane in silicon. Reconstruction implies a high migration energy E_m, since it requires the breaking and reforming of bonds for kink motion. Experiments [14] give $E_m \geq 1.2$ eV for 60° and edge dislocations.

Electron microscope (TEM) images show that dislocations in silicon are dissociated into partial dislocations, separated by a ribbon of stacking fault (SF), as shown schematically in Fig. 1. "Forbidden reflection" TEM lattice images, at 0.33 nm resolution suggest fine kinklike directional fluctuations [15]. Dislocation motion results if thermal fluctuations throw a segment of line forward, generating kinks such as A in Fig. 1, which are driven apart along the line by the application of an external stress. Measurements of dislocation velocity by TEM, intermittent loading, internal friction [5] give $1.8 < Q < 2.5$ eV for the sum of kink mobility and nucleation energies. We chose a centric supercell with 186 Si atoms and two 30° partial dislocations forming a dipole, as shown in Fig. 1. The driving force for kink motion is the tendency for the dipole to annihilate, which provides a stress on each dislocation of about 198 MPa (SF energy $\gamma = 76$ ergs/cm^2 [16]). Each partial contains a kink (opposite signs), and the monoclinic supercell is periodically continued without severe bond distortion. Lateral alignment of kinks minimizes kink-kink forces. The structure corresponds to a line of geometric kinks running 10.82° away from [1–10] and

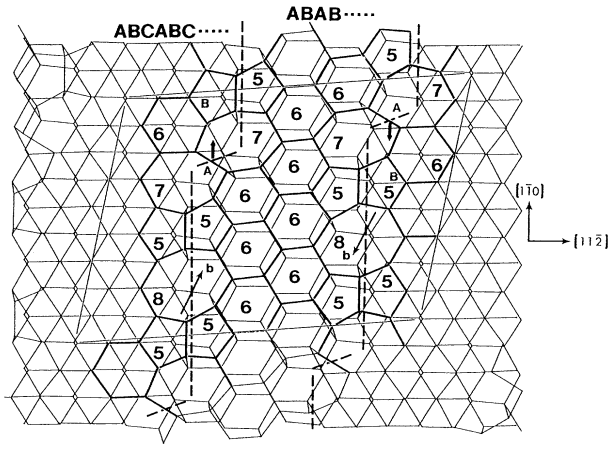

FIG. 1. Projection down (111) of atomic structure of reconstructed 30° partial dislocation with kinks at A. Dotted lines trace dislocation cores. Unit cell used for calculations and stacking sequences indicated. N-membered rings in middle layer (bold lines) numbered.

 0031-9007/95/74(17)/3392(4)$06.00

was partly derived from high resolution electron micrographs [17]. Since reconstruction is favored [18–20] we adopt Hirsch's model [6] for the kink, and do not consider antiphase defects, which may be rare [5]. We denote the initial state of the kink by A and the final state, in which it has moved one period along the line, by B (Fig. 1).

An approximate first-principles electronic structure method [21] is used that closely matches more rigorous calculations, but greatly reduces computational effort. Several applications have been reported, including surface reconstructions, clathrate structures, and fullerenes [22]. Total energy E_{tot} equals a sum of single-electron eigenvalues (E_{BS}), and electron-electron interaction energy and an ion-ion interaction energy (E_{SR}, short range), and an exchange-correlation energy correction E_{XC} based on the local density approximation [21]. The pseudopotential is a nonlocal norm-conserving Hamann-Schluter-Chiang type [23]. The wave function is approximated as a linear combination of pseudoatomic orbitals, obtained from self-consistent local density approximation pseudopotential computations for isolated atoms with cutoff radius $r_c = 5$ bohr. Our fast algorithm used neutral-atom charge densities in the evaluation of the electron exchange-correlation energy (Harris functional [24]). Our quantum molecular dynamics (QMD) algorithm obtains the force on the ith atom from the derivative of total energy with respect to nuclear coordinates. Atoms move in 2 fs time steps according to classical equations of motion; the minimum internal energy state is sought using a dynamical quenching algorithm. Several empirical potentials were also evaluated [25–28]. Four fully relaxed reconstructed kink structures were first obtained using these potentials in combination with MD. Each relaxed structure was compared with the *ab initio* method. Our results [29] show that the lowest energy structure for the 30° partial with kinks is obtained using the Tersoff Si(c) potential, which gives a lower bond bending stiffness than others [30]. Bigger *et al.* [12] have shown that the Tersoff potential also reproduces the *ab initio* structure well for a reconstructed 90° partial dislocation. We therefore adopted this Tersoff fully relaxed structure as the initial structure and continued to relax it using the *ab initio* QMD technique. Two special k points along the direction of the geometric kink are used. After relaxation, a stable configuration with an average atomic force close to zero (~0.25 eV/Å per kink) was obtained (kink A). A second similar computation (kink B) was completed for the same structure in the final state, with the kink positions incremented (from A to B) by 1 a.u. To investigate the pathway and barrier between states A and B, we adopt a configuration coordinate point of view, assuming all atoms move on straight line paths between these configurations. The *ab initio* algorithm is used to obtain the total energy per kink as a function of the configuration coordinate along this line. Since the use of a straight line path overestimates the saddle-point energy (the average atomic force obtained for the straight line saddle point is twice as large as that of kink A), we subsequently applied a constrained MD relaxation, in which kink core atoms with large motions (≥0.4 Å) were fixed at the saddle-point configuration given by the straight path algorithm. Relaxation was terminated when forces at the saddle point were equal to those of the relaxed kinks. Results are shown in Fig. 2. The energy of kink B is higher than that of kink A because of the slightly higher force (~0.03 eV/Å per kink) and of the additional stacking fault. Kinks therefore tend to move from B to A. We identify the height of the barrier (moving from B to A) as the kink migration energy $E_m = 2.1 \pm 0.3$ eV (rounding error only). This value is close to the experimental value of 1.58 ± 0.22 eV in n-type silicon [31], and to theoretical values between 1.4 and 1.9 eV [32], depending on the kink variant considered. We now consider the electronic structure associated with kink motion. Since we use only sp^3 orbitals, the band gap of bulk Si in our model is larger (~1.7 eV) than the experimental gap of Si (1.17 eV at 0 K). Figure 3 shows the band structures for (a) kink A, (b) the saddle point of the reconstructed kink, and (c) the final kink state B. The filled valence charge density on the midplane for kink A viewed along [111] is shown in Fig. 4. Whereas it is generally accepted [13] that the Si band gap is cleared of deep states due to straight dislocation cores by Peierls-type reconstruction for both the common 30° and 90° partial dislocations, we find that several semiconducting deep states occur once kinks are introduced along the dislocation line. In particular, we find that the saddle-point kink configuration is metallic, whereas the initial and final states A and B are semiconducting with a small gap. The total energy at the saddle point can be written as a sum of E_{BS}, E_{SR},

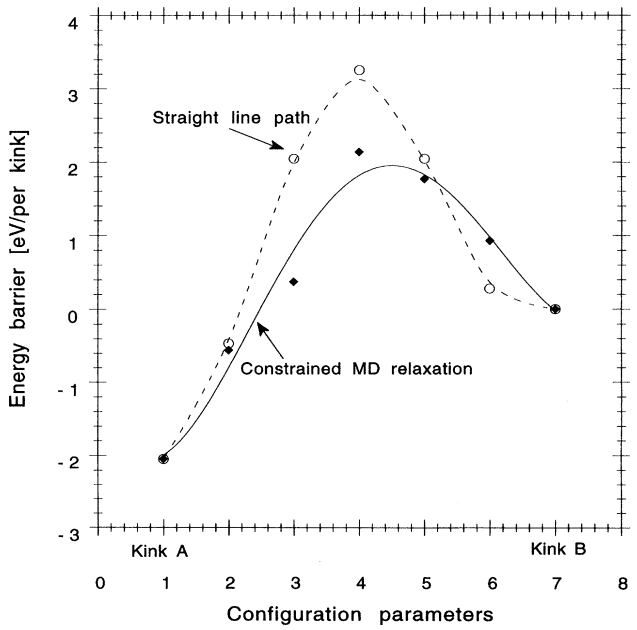

FIG. 2. Total internal energy change per kink plotted as a function of configuration parameter for kink migration.

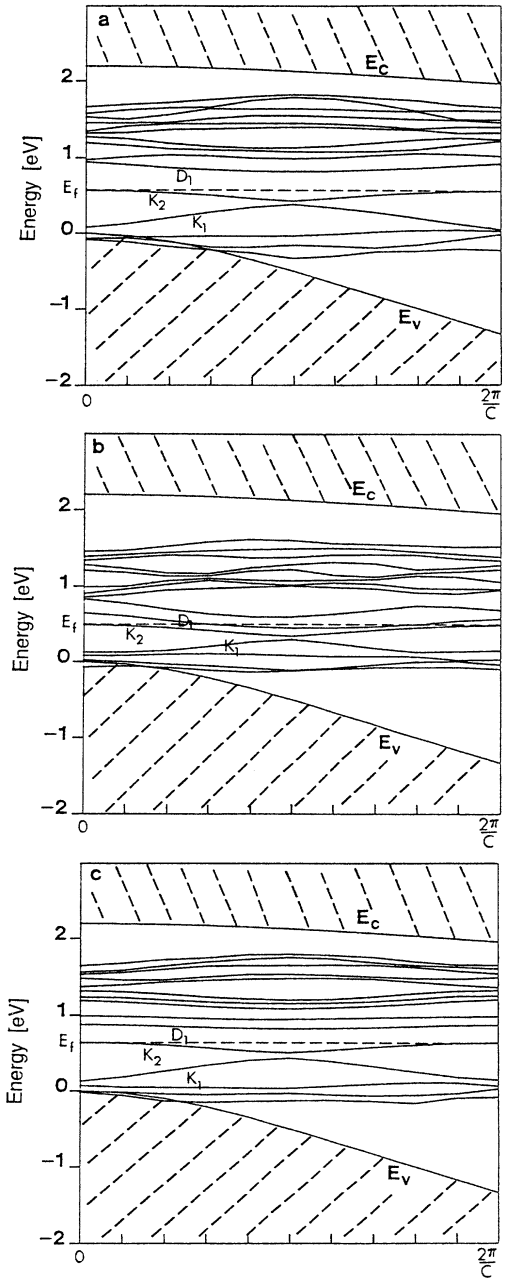

FIG. 3. Band structures for (a) kink at position A, (b) saddle-point configuration, and (c) kink at B. Bulk band structure shaded. Metallic defect states are formed at the saddle point as the kink moves into the next secondary Peierls valley. c is the period along the line of kinks.

and E_{XC} [21]. Changes in these terms between the saddle point and A and B states were compared. We find that the energy barrier arises mainly from changes ΔE_{BS} in the band structure energy E_{BS}. ($\Delta E_{SR} = \Delta E_{BS}/6$, $\Delta E_{XC} \approx 0$). To illustrate the energy change between the saddle point and the stable kink, we assume that changes in the density of states (DOS) occur only in the gap region. Thus, we assume that the DOS $n(\varepsilon)$ and energy

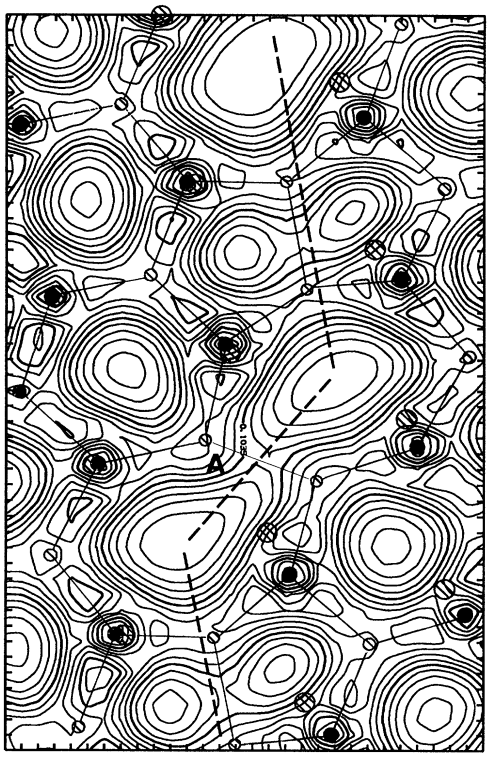

FIG. 4. Charge density map on (111) for kinks with $k = \pi/c$. Contours of constant charge density are given in units of $744e/V_c$, with V_c the unit cell volume.

levels ε below the bulk valence band maximum E_v do not change for both the saddle point and the stable kink. Then, the energy barrier for kink motion can be regarded as the energy difference due to the change of all occupied defect states between the saddle-point configuration and the stable kink, as suggested by Jones [33] and Hirsch [6]. The change in band structure energy is then

$$\delta E_{BS} = \int_{E_v}^{E_f} f(\varepsilon) n^s(\varepsilon) \varepsilon \, \delta\varepsilon - \int_{E_v}^{E_f} f(\varepsilon) n^A(\varepsilon) \varepsilon \, \delta\varepsilon, \quad (1)$$

where $f(\varepsilon)$ is the Fermi distribution function and $n^s(\varepsilon)$, $n^A(\varepsilon)$ are the density of states for the saddle point and kink geometry A, respectively.

The position of the Fermi level in Eq. (1) indicates the sensitivity of these states to doping effects, which shift the Fermi energy. To interpret the effect of doping on the energy barrier for kink motion, we rewrite Eq. (1) for n-doped silicon as

$$\delta E_{BS}^{n\text{-type}} = \delta E_{BS} + \left\{ \int_{E_f}^{E_f^{n\text{-type}}} n^s(\varepsilon) \varepsilon \, d\varepsilon - \int_{E_f}^{E_f^{n\text{-type}}} n^A(\varepsilon) \varepsilon \, d\varepsilon \right\}. \quad (2)$$

This expression incorporates all strain effects through the electronic structure and includes the doping effect through

the states in the gap, as in the Jones model [33]. If the defect states above the intrinsic Fermi level E_f move down at the saddle-point configuration, then a reduced energy barrier is obtained due to n doping. In Fig. 3(a) we see that for intrinsic Si, kink states K_1 and K_2 are occupied, and defect state D_1 is unoccupied. At the saddle point, the defect state D_1 comes down to lie below the Fermi level. If state D_1 were occupied due to n doping, the barrier would be reduced. Similarly in p material, if states K_1 or K_2 below E_f move up at the saddle point, but are unoccupied because of doping, the barrier height for the kink motion will be reduced. Although not seen in Fig. 3, we have confirmed this behavior by numerical calculation. (For example, an increase of 0.53 eV from kink A to saddle point at $k = \pi/c$.) Thus, the movement of the defect gap states at the saddle point controls the effect of doping on the energy barrier for dislocation motion. If on the other hand the unoccupied (occupied) defect states were to become higher in energy at the saddle point, an increased energy barrier for n-type (p-type) doping would be predicted. These calculations support the well known result [34] that doping enhances dislocation mobility in silicon, n doping moreso than p. For germanium, dislocation velocity increases with n-type doping and decreases with p-type doping. We therefore speculate that in Ge the unoccupied defect states become deeper at the saddle point, whereas the occupied defect states become shallower.

Finally, we note that in previous work [35] on the atomic energy barrier to crack propagation in silicon, a delicate balance between the Coulomb energy E_{SR} and band structure energy E_{BS} was found to be controlling, with the Coulomb interaction providing the retarding force. Experimentally [36], doping has little effect on the fracture toughness of silicon, consistent with its small effect on E_{BS}. Coulomb interactions come into play for the large tensile bond stretchings involved in fracture, by comparison with the shearing motions involved in kink movement. The Si(111)-(2 × 1) shuffle surface reconstruction generated by cleavage may be governed by the Coulomb force, whereas the glide movement for dislocations is controlled by the band structure force.

We express thanks to P. Rez, H. Kolar, A Demkov, and H. Alexander. This work was supported by NSF Grant No. DMR916362.

[1] J. P. Hirth and J. Lothe, *Theory of Dislocations* (McGraw-Hill, New York, 1982).
[2] J. R. Patel and A. R. Chaudhuri, Phys. Rev. **143**, 601 (1966).
[3] L. C. Kimerling, J. R. Patel, J. L. Benton, and P. E. Freeland, in *Proceedings of the International Conference on Defects and Radiation Effects in Semiconductors, Osio, Japan, 1980* (Institute of Physics, Bristol, 1981), Vol. 59, p. 11.
[4] M. Duesbery and G. Richardson, Solid State Mater. Sci. **17**, 1 (1991).
[5] H. Alexander and H. Teichler, in *Materials Science and Technology,* edited by R. W. Cahn, P. Hassen, and E. J. Kramer (VCH Weinheim, Cambridge, 1993), Vol. 4, p. 251.
[6] P. B. Hirsch, Mater. Sci. Tech. **1**, 666 (1985).
[7] M. Heggie and R. Jones, Inst. Phys. Conf. Ser. **67**, 1 (1983).
[8] P. B. Hirsch, J. Microsc. **118**, 3 (1980).
[9] F. Louchet and J. Thibault-Desseaux, Rev. Phys. Appl. **22**, 207 (1987).
[10] H.-J. Möller, Acta Metall. **26**, 963 (1978).
[11] M. Heggie, R. Jones, and A. Umerski, Phys. Status Solidi (a) **138**, 383 (1993).
[12] J. Bigger, D. McInnes, A. Sutton, M. Payne, I. Stich, R. King-Smith, D. Bird, and L. Clark, Phys. Rev. Lett. **69**, 2224 (1992).
[13] J. R. Chelikowsky, Phys. Rev. Lett. **49**, 1569 (1982).
[14] B. Ya. Farber, Yu. L. Iunin, V. I. Nikitenko, H. Alexander, and P. Specht, Phys. Status Solidi (a) **138**, 557 (1993); and earlier papers.
[15] H. Alexander, J. Spence, D. Shindo, H. Gottschalk, and N. Long, Philos. Mag. A **53**, 627 (1986).
[16] J. C. H. Spence and H. Kolar, Philos. Mag. A **39**, 59 (1979).
[17] J. C. H. Spence, in *Proceedings of the 39th Annual Meeting of the Electron Microscopy Society of America, Atlanta, Georgia, 1981,* edited by G. Bailey (Claitor's Publishing Division, Baton Rouge, LA, 1981), p. 120.
[18] R. Jones, J. Phys. (Orsay) Suppl. 6 **40**, C6-33 (1979).
[19] S. Marklund, J. Phys. (Orsay) Suppl. 9 **44**, C4-25 (1983).
[20] J. E. Northrup, M. L. Cohen, J. R. Chelikowsky, J. C. H. Spence, and A. Olsen, Phys. Rev. B **24**, 4623 (1981).
[21] O. F. Sankey and D. J. Niklewski, Phys. Rev. B **40**, 3979 (1989).
[22] G. Adams and O. Sankey, Phys. Rev. Lett. **67**, 867 (1991), and references therein.
[23] D. R. Hamann, M. Schlüter, and C. Chiang, Phys. Rev. Lett. **43**, 1494 (1979).
[24] J. Harris, Phys. Rev. B **31**, 1770 (1985).
[25] J. Tersoff, Phys. Rev. B **38**, 9902 (1988).
[26] B. W. Dodson, Phys. Rev. B **35**, 2795 (1987).
[27] E. Kaxiras and K. C. Pandey, Phys. Rev. B **38**, 12 736 (1988).
[28] H. Koizumi and T. Ninomiya, J. Phys. Soc. Jpn. **44**, 898 (1978).
[29] Kaxiras, Keating, and Dodson were 2.85, 12.5, and 1.43 eV/cell higher than the Tersoff potential.
[30] U. Trinczek and H. Teichler, Phys. Status Solidi (a) **137**, 577 (1993).
[31] V. Nikitenko, B. Farber, and Yu. Iunin, Sov. Phys. JETP **66**, 738 (1987).
[32] R. Jones, in *Dislocations in Solids,* edited by H. Suzuki *et al.* (University of Tokyo Press, Tokyo, 1985), p. 343.
[33] R. Jones, Philos. Mag. B **42**, 213 (1980).
[34] J. R. Patel and A. R. Chaudhuri, Phys. Rev. **143**, 601 (1966).
[35] J. C. H. Spence, Y. M. Huang, and O. F. Sankey, Acta Metall. **41**, 2815 (1993).
[36] G. C. Rybicki and P. Pirouz, NASA Technical Paper No. 2863 (1988); T. Michalski, Y. M. Huang, and J. Spence (unpublished).